

# Magnetic Properties of the low dimensional spin system (VO)<sub>2</sub>P<sub>2</sub>O<sub>7</sub>: ESR and susceptibility

A. V. Prokofiev, F. Büllersfeld, W. Assmus, H. Schwenk, D. Wichert, U. Löw, B. Lüthi  
*Physikalisches Institut, Universität Frankfurt, Robert Mayer Str. 2-4, D-60054 Frankfurt*

## Abstract

Experimental results on magnetic resonance (ESR) and magnetic susceptibility are given for single crystalline (VO)<sub>2</sub>P<sub>2</sub>O<sub>7</sub>. The crystal growth procedure is briefly discussed. The susceptibility is interpreted numerically using a model with alternating spin chains. We determine  $J=51$  K and  $\delta=0.2$ . Furthermore we find a spin gap of  $\approx 6$  meV from our ESR measurements. Using elastic constants no indication of a phase transition forcing the dimerization is seen below 300 K.

## I. INTRODUCTION

The interest in low dimensional spin systems is motivated by the occurrence of many different ground states and of excitations with spin gaps. Prominent examples are compounds with spin chains exhibiting Spin-Peierls transitions, or dimerisation due to nearest and to next nearest exchange interactions or Spin 1 systems. In addition spin ladders show also unexpected results<sup>1</sup>.

The magnetism of the compound  $(\text{VO})_2\text{P}_2\text{O}_7$  (abbreviated VOPO) experienced quite different interpretations. The first susceptibility measurements on polycrystalline material<sup>2</sup> were interpreted with an alternating chain model and a two leg ladder model<sup>3</sup>. Subsequent inelastic neutron scattering data indicating a spin gap of about 50K were used as indication of a ladder model<sup>4</sup>. Recently neutron scattering experiments on an arrangement of many (200) tiny single crystals (dimensions  $< 1\text{mm}^3$ ) gave evidence of strong dispersion in the b-direction of this orthorhombic compound (see Fig. 1) thereby eliminating the two leg ladder model and installing again the alternating chain model<sup>5</sup>. Our previous susceptibility and magnetic resonance work on polycrystalline VOPO was interpreted with the two leg ladder model<sup>6,7</sup>.

Recently we succeeded in growing large single crystals in excess of  $1\text{mm}^3$ . We present in this paper a brief description of the crystal growth procedure and we present magnetic resonance (ESR) and susceptibility data for these single crystals as a function of temperature and magnetic field. We give an interpretation of our results using the alternating chain model<sup>5</sup>.

## II. EXPERIMENT

The growth of single crystals of VOPO is complicated by two features of this compound. The first is the strong sensitivity of the oxidation state of Vanadium (and of the stability of VOPO) to the oxygen content in the growth atmosphere. The second is the tendency of VOPO-melt to a glass formation during cooling due to the high viscosity. Therefore the growth has to be carried out in an atmosphere with strictly controlled oxygen content and with a very low growth rate.

VOPO powder for the growth was prepared by thermal decomposition of the precursor  $(\text{VO})\text{HPO}\cdot 5\text{H}_2\text{O}$  in argon flow at  $700^\circ\text{C}$ . The precursor was synthesized according to Centi et al.<sup>8</sup>. Single crystals were grown by pulling with the velocity of  $2\text{mm/day}$  from the melt with simultaneous cooling of the melt with the rate  $4\text{--}8\text{ K per day}$ . Single crystals with sizes up to  $10 \times 3 \times 3\text{ mm}^3$  have been grown in a week. The details of the growth technique will be published elsewhere<sup>9</sup>.

Growth atmosphere with various oxygen contents were used. The latter varied in the limits  $0.2\text{--}0.6\text{ vol\%}$  for different runs. This concentration regions provide the stability of the phase  $(\text{VO})_2\text{P}_2\text{O}_{7+x}$ , which has a homogeneity range in oxygen content<sup>10</sup>. This, however, requires the determination of the oxygen content (or the Vanadium oxidation state) in the growth crystals. Thermogravimetric analysis based on the reactions of either oxidation of  $(\text{VO})_2\text{P}_2\text{O}_{7+x}$  up to  $\text{VPO}_5$  or mild reduction in vacuum to stoichiometric composition

(VO)<sub>2</sub>P<sub>2</sub>O<sub>7</sub> showed that the Vanadium oxidation state in these conditions varied in the limits 4.0 – 4.4.

We measured the susceptibility either with a vibrating sample magnetometer or as magnetization in a constant field of  $1 - 2T$ . Both methods gave the same results. An absolute calibration was performed with a Faraday balance. For the magnetic resonances we used various diodes in the frequency range 130 – 300 GHz in combination with frequency multipliers<sup>11</sup>.

### III. RESULTS AND DISCUSSION

#### A. Resonance

In Fig. 2 we first present magnetic resonance results in the frequency region 134 - 288 GHz. In the three crystallographic directions a,b,c we find Zeeman split lines with g-factors  $g_a = 1.937$ ,  $g_b = g_c = 1.984$ . Comparing these g-factors with previous results on polycrystalline specimens<sup>6</sup> ( $g^{\parallel} = 1.94$ ,  $g^{\perp} = 1.98$ ) we note the good agreement of the latter values with the present ones. This gives a clear indication of the successful averaging procedure to obtain the lineshape in the polycrystalline material. In addition we see some small resonances in the single crystal similar to the resonance form seen in Ref. 6. Details will be discussed elsewhere. In the polycrystalline sample the total absorption of the ESR line could be fitted to a singlet triplet energy gap of 150 K (see Ref. 7). We have assumed that this temperature behaviour could arise from transitions at  $k=0$ . In the polycrystalline material an energy gap of this size was observed in inelastic neutron scattering<sup>4</sup>.

For the single crystal resonances of Fig. 2 arise from excited triplet excitations too, as shown in Fig. 3. Here the total absorption strength for a resonance of 134 GHz is shown as a function of temperature. The full line indicates the calculated intensity of an excitation within the triplet with a fitted singlet-triplet gap of 1374 GHz = 67K. This gives a satisfactory description of the absorption. This energy gap fits to the upper mode of the measured excitation spectra<sup>5</sup>. The small dispersion in the c-direction gives an enhanced density of states for such a resonance. The dotted curve gives an analogous fit for an excitation of 849GHz = 36K corresponding to the lower observed branch of Ref. 5. This curve does not fit the experimental results at all. An alternating chain model, discussed in section III C, with  $J = 51K$  and  $\delta=0.2$  gives a gap of 58K ( see Ref. 14) close to the observed one of 67K. More detailed information of the excitation spectra are needed to reach a final conclusion for the observed triplet excitation.

#### B. Susceptibility

In Fig. 4a we present the susceptibility. The curves along the different axis are slightly different. They all have a maximum at  $74 \pm 2K$  close to the broad maximum observed for the polycrystalline specimens<sup>2,6</sup>.

The remarkable feature of the single crystal result is however the almost total absence of a low temperature tail compared to the previous polycrystal work (compare e.g. the inset of Fig.1 in Ref. 6 with our results in Fig. 4a). In the polycrystalline material we could fit the defect part of the susceptibility to a  $T^{-0.54}$  law. In the single crystal measurements it is not possible to fit a law to the defect part of the susceptibility because the temperature region is too small. This defect part is due to chain ends or paramagnetic  $V^{4+}$  ions which are isolated by nonmagnetic  $V^{5+}$  ions. In the inset of Fig. 4a we show 2T and 10T ( $\chi = M/B$ ) susceptibility data. For the high field data the low temperature tail is completely suppressed as expected.

The difference in the temperature dependence of the susceptibility for the different crystallographic directions is mainly due to the different g-factors. The g-factor for the  $\langle 100 \rangle$  direction is smaller than the g-factors for the other directions as discussed above. This is similar to the findings of Ref. 6 and to the ESR measurements as pointed out above. The absolute value of the maximum of the susceptibility is about  $2 * 10^{-3}$  emu/molV. These values are slightly higher than the maximum value of  $\chi(T)$  in Ref. 2 because in our single crystal samples the valence state of the V-ions is closer to 4+. There are more magnetic ions that contribute to the susceptibility of the chains.

To fit a Curie law to the susceptibility data one had to measure to higher temperatures than 230K. The Curie-Weiss law for the  $\langle 010 \rangle$  direction gives an approximate Curie constant of  $C = .374$  emu/molV and an upper limit of a Curie Weiss temperature of  $-70K$ .  $C$  gives an effective Spin per ion of  $S = 1/2$  if we take the g-factor of  $g = 1.984$  from above. So the susceptibility gives also a valence of about 4.0 for the V-ions similar to the oxidation reactions.

### C. Discussion of the susceptibility

We now analyse the susceptibility measurement quantitatively in the framework of the spin 1/2 Heisenberg model with alternating couplings given by the Hamiltonian

$$H = 2J \sum_{i=1}^N \left\{ (1 + \delta(-1)^i) \vec{S}_i \vec{S}_{i+1} \right\}. \quad (3.1)$$

We determined  $J$  by comparing the experimentally found temperature  $T_{max} = (74 \pm 2)K$  where  $\chi$  has its maximum with the theoretical result for  $T_{max}/J$  from exact diagonalization. For a successful application of this approach see Ref. 13. Subsequently we used  $J(\delta)$  to calculate the maximum  $\chi_{max} = \chi(T_{max})$  of the susceptibility in emu/molV as a function of  $\delta$ . The results are shown in Fig. 5a and 5b respectively. From the experimental value  $\chi_{max} = 2.07 * 10^{-3}$  emu/molV with  $g = 2$  and with  $T_{max}=74K$  we find  $\delta = 0.2$  and  $J = 51K$ . The calculated susceptibility for these parameters together with the experimental result in the  $\langle 010 \rangle$  direction are shown in Fig. 4b. Note that no defect part is subtracted as mentioned in section IIIB. This explains the less good agreement for  $T < T_{max}$ .

The maxima used in Fig. 5 are obtained by exact diagonalization of the complete Hamiltonian for up to 16 spins and  $\delta = 0.0...1.0$ . Finite size effects do not play a role in the

temperature range of  $T_{max}$ . This can be seen from Fig 5a and b where the results for chains with N=14 and 16 spins fall together.

We point out that the influence of an additional frustrating interaction  $2J \sum_{i=1}^N \alpha S_i S_{i+2}$  shifts the maximum of the susceptibility to smaller temperatures  $T/J$  and consequently for the same experimental  $T_{max}$  we obtain larger values for the coupling J. The absolute value of  $\chi$  is lowered both by the frustration, and by the scaling factor  $1/J$  (see Ref. 12).

In Fig. 6 we show the elastic constant  $c_{11}$  as a function of temperature. The absolute value of the sound velocity is 5097 m/s at 4.2K. No indication of a phase transition is observed for  $T \leq 300$ K. A discussion of the different elastic constants will be given later.

In conclusion we have performed susceptibility and ESR measurements on single crystalline samples. Based on a model of a dimerized chain we calculated  $J=51$ K and  $\delta=0.2$ . Our ESR-measurements show a singlet-triplet gap of 67 K in good agreement to the upper gap as measured in inelastic neutron scattering. The elastic constant  $c_{11}$  shows that the dimerization is not due to a phase transition. Further work has to investigate the details of the ESR-Signal and to estimate the influence of possible interchain exchange interactions (as seen in Ref. 5).

#### Acknowledgement

This research was supported in part by SFB 252. We thank G. Bouzerar, K. Fabricius, A. P. Kampf and G.S. Uhrig for enlightening discussions.

## REFERENCES

- <sup>1</sup> E.Dagotto, T.M.Rice, Science 271, 618 (1996)
- <sup>2</sup> D.C.Johnston, J.W.Johnson, D.P.Gashorn, A.J.Jacobson, Phys.Rev.B35, 219(1987)
- <sup>3</sup> T.Barnes and J.Riera, Phys.Rev.B50, 6817(1994)
- <sup>4</sup> R.S.Eccleston, T.Barnes, J.Brody, J.W.Johnson, Phys.Rev.Lett. 73, 2626(1994).
- <sup>5</sup> A.W.Garrett et al., Phys.Rev.Lett. 79,745(1997)
- <sup>6</sup> H.Schwenk, M.Sieling, D.König, W.Palme, S.A.Zvyagin, B.Lüthi, R.S.Eccleston Solid State Comm. 100, 381(1996)
- <sup>7</sup> H.Schwenk, D.König, M.Sieling, S.Schmidt, W.Palme, B.Lüthi, S.A.Zvyagin, R.S.Eccleston, M.Azuma, M.Takano Physica B 237-238, 115(1997)
- <sup>8</sup> G.Centi, F.Trifiro, G.Poli, Appl.Catal. 19,225(1985).
- <sup>9</sup> A.V.Prokofiev, F.Büllesfeld, W.Assmus, Crystal Research and Tech.-(to be publ.).
- <sup>10</sup> M.Lopez, Granados, J.C.Conesa, M.Fernandes-Garcia, J.Catal. 141,671(1993)
- <sup>11</sup> W.Palme et al., Z.Phys.B92, 1(1993)
- <sup>12</sup> U.Löw to be published
- <sup>13</sup> K.Fabricsius, A.Klümper, U.Löw, B.Büchner, T.Lorenz, G.Dhalenne, A.Revcolevschi, to appear in Phys.Rev.B57,(1998)
- <sup>14</sup> G.S.Uhrig, H.J.Schulz, Phys.Rev.B54, 54(1996)

Fig. 1:

Schematic description of the structure and magnetic interactions in VOPO, adapted from Ref. 5

Fig. 2:

Resonance frequencies versus magnetic field for the different crystallographic directions.

Fig. 3:

Absorption strength of the 134 GHz line as a function of temperature. The full and dotted lines are fits for a resonance within the triplet state as explained in the text.

Fig. 4a:

Temperature dependence of magnetic susceptibility in VOPO for the different crystal directions. In the inset we give the low temperature susceptibility ( $\chi=M/B$ ) for 2T and 10T.

Fig. 4b:

Temperature dependence of magnetic susceptibility in VOPO for the  $\langle 010 \rangle$  direction (open circles) and calculated susceptibility with  $J=51\text{K}$  and  $\delta=0.2$  (full line).

Fig. 5:

a) Antiferromagnetic exchange coupling  $J(\delta)$ .

b) Maximum susceptibility  $\chi_{max}(\delta)$  normalized to  $g = 2$ .

$T_{max}=72\text{K}$  (squares),  $74\text{K}$  (circles),  $76\text{K}$  (triangles). Small filled symbols for  $N = 14$ , large open symbols for  $N = 16$ .

Fig. 6:

Relative sound velocity for the  $c_{11}$ -mode.

Absolute sound velocity for the  $c_{11}$ -mode:  $v=5097\text{m/s}$  at  $T = 4.2\text{K}$ .

Fig. 1

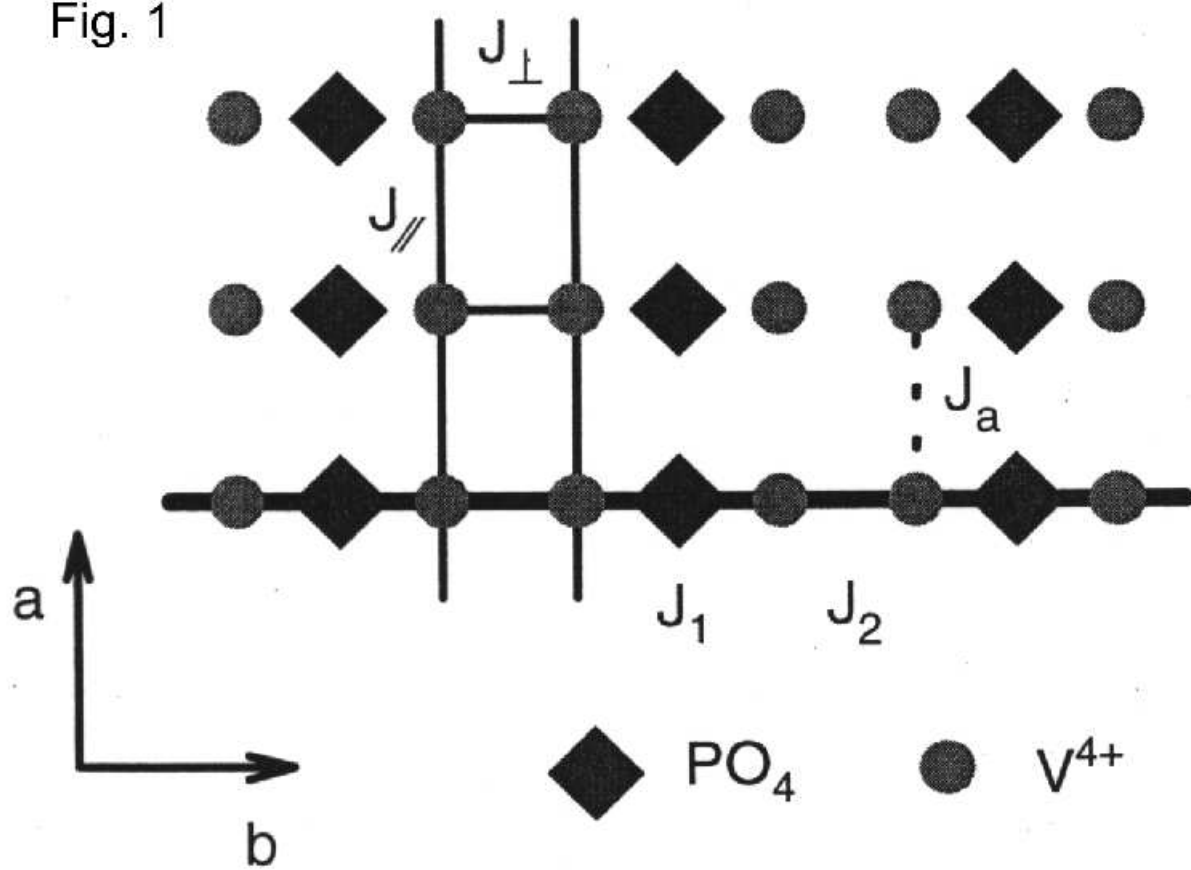




Fig. 2

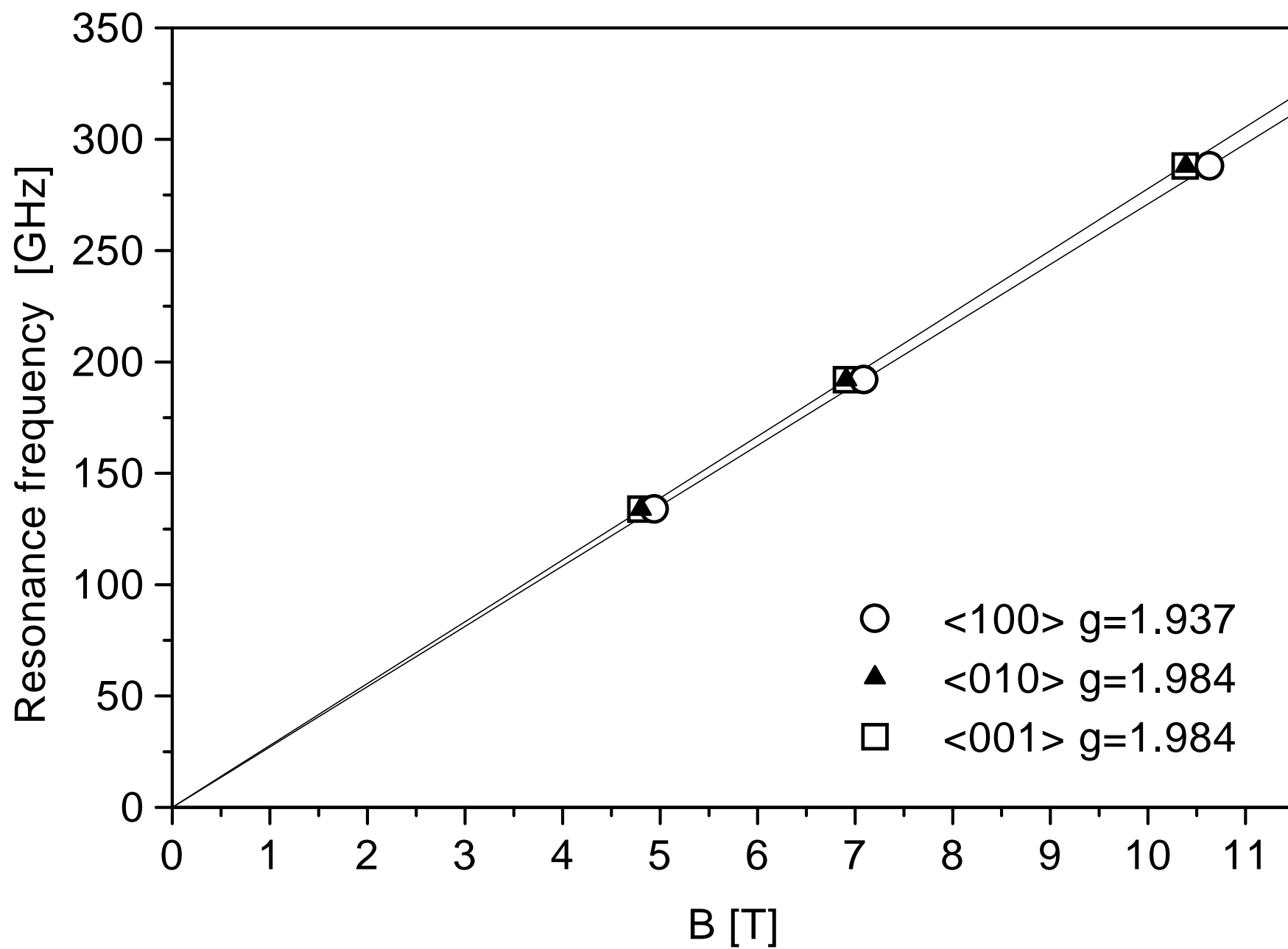


Fig. 3

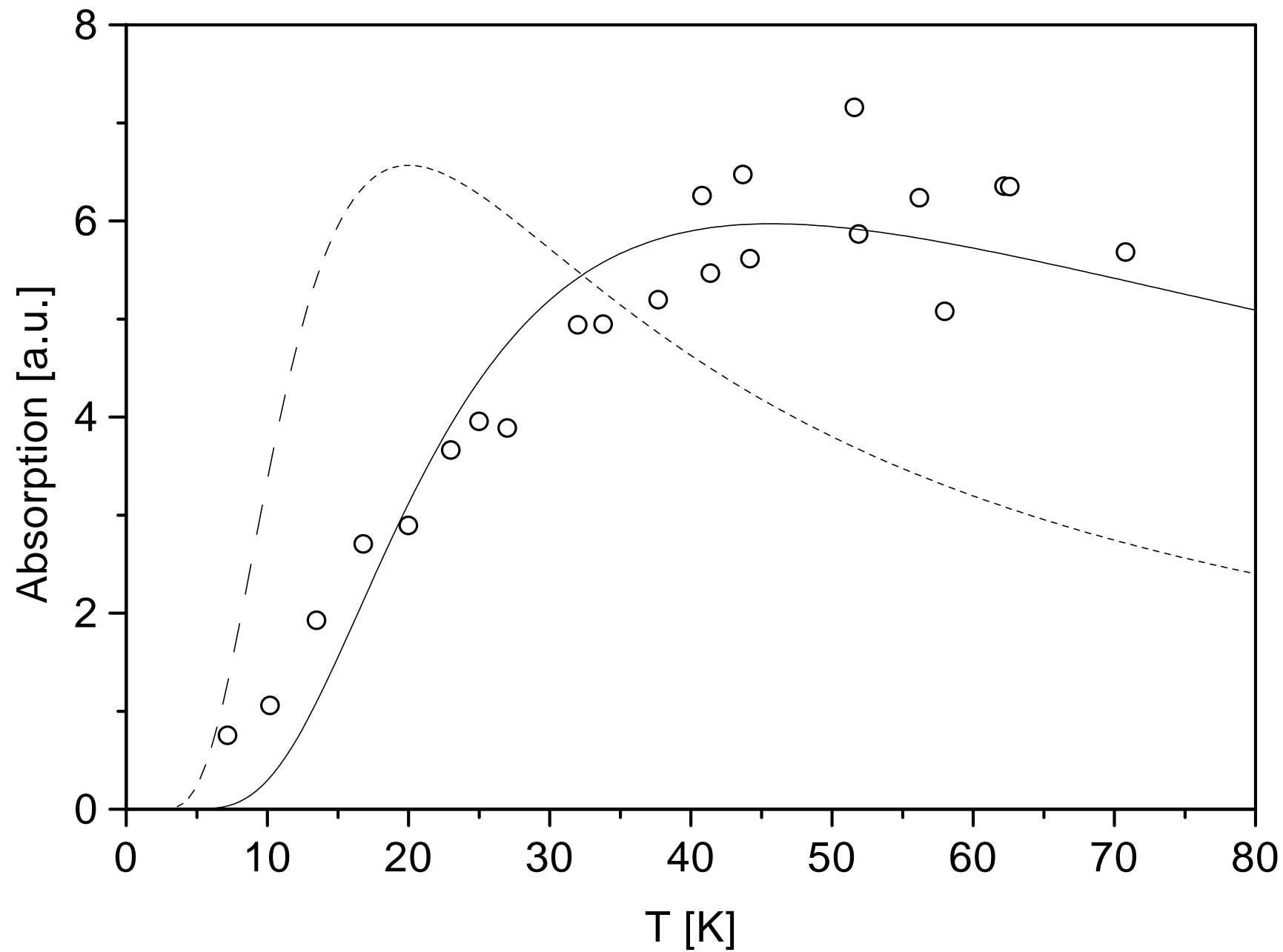


Fig. 4a

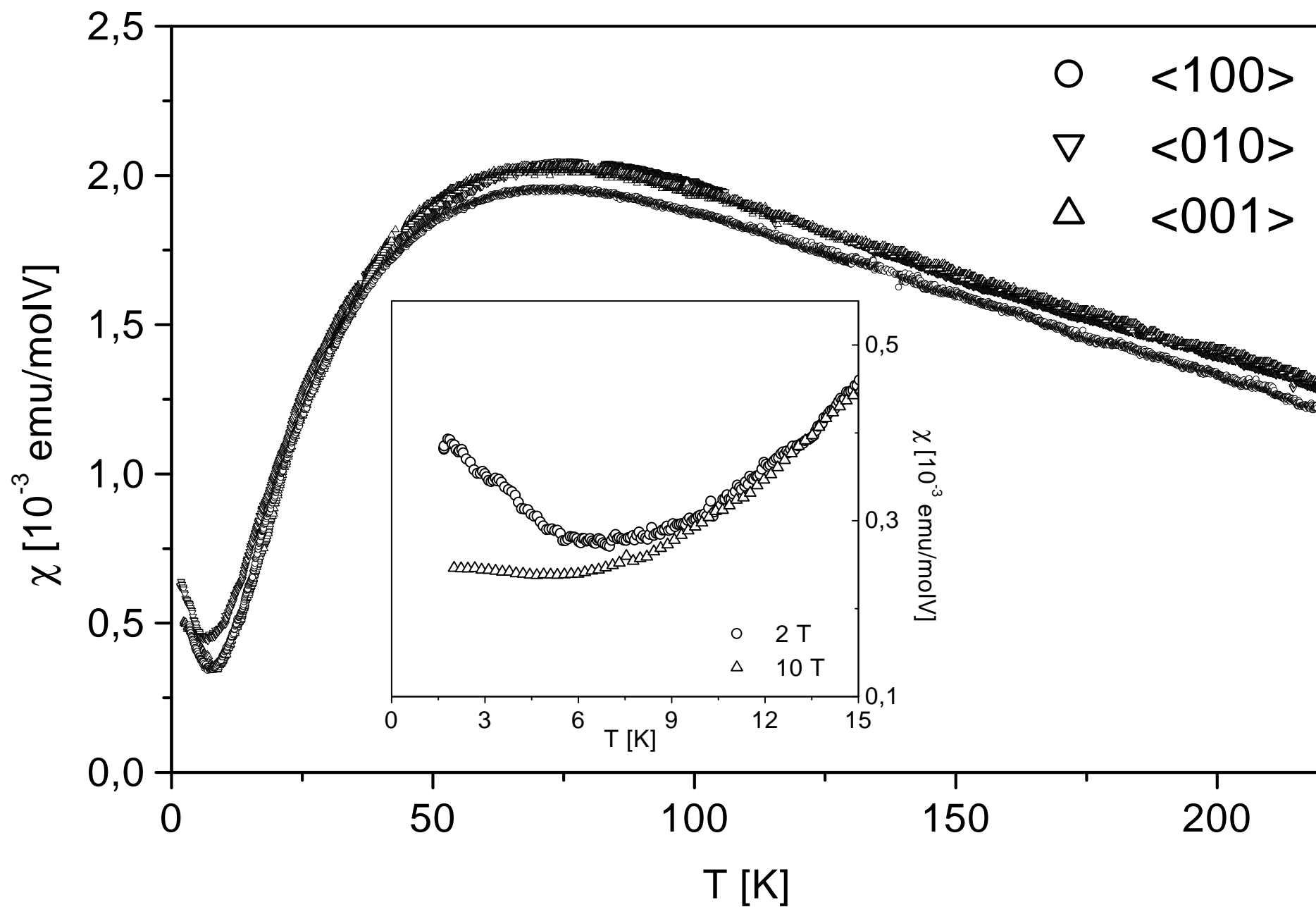


Fig. 4b

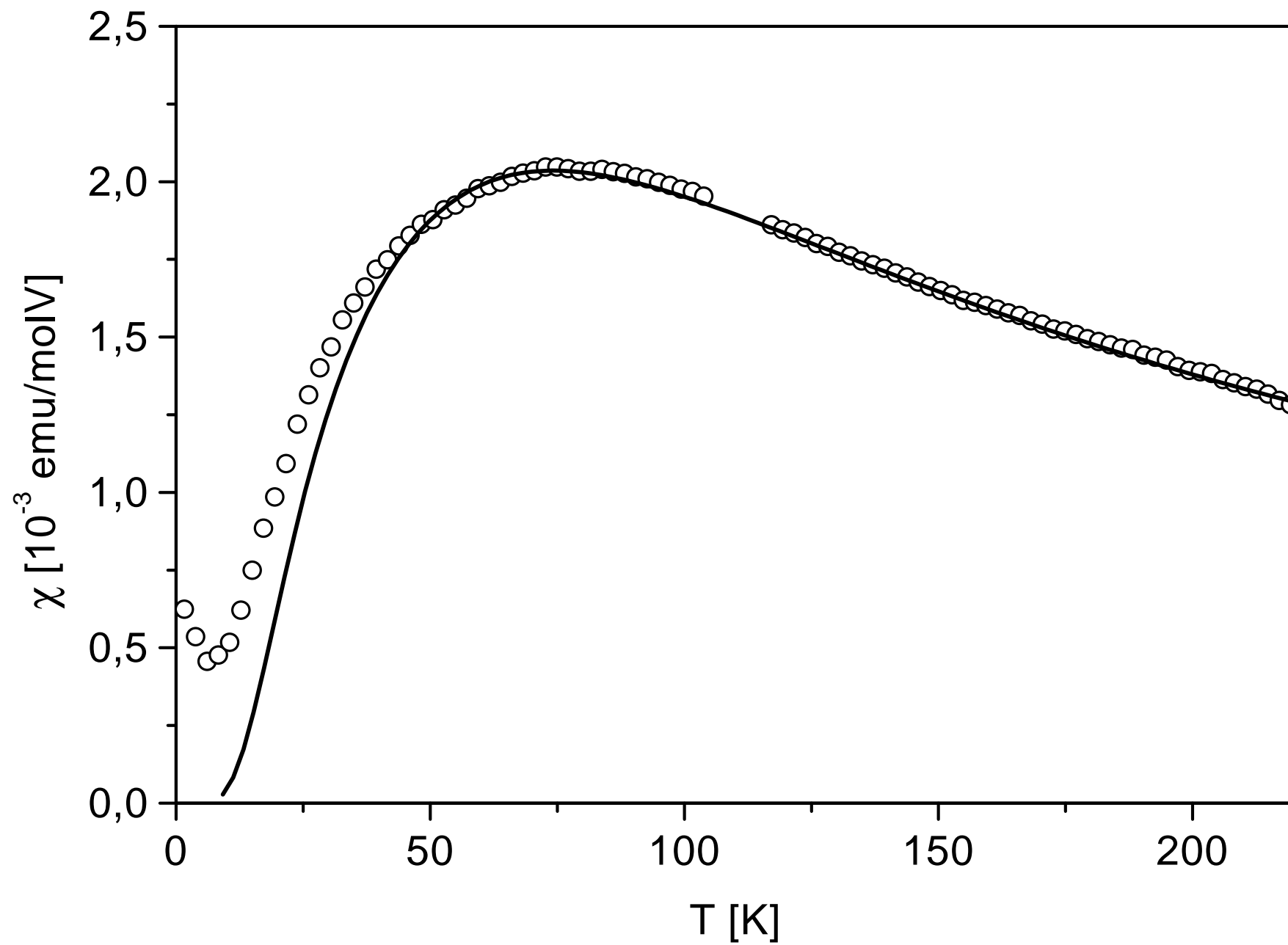


Fig. 5

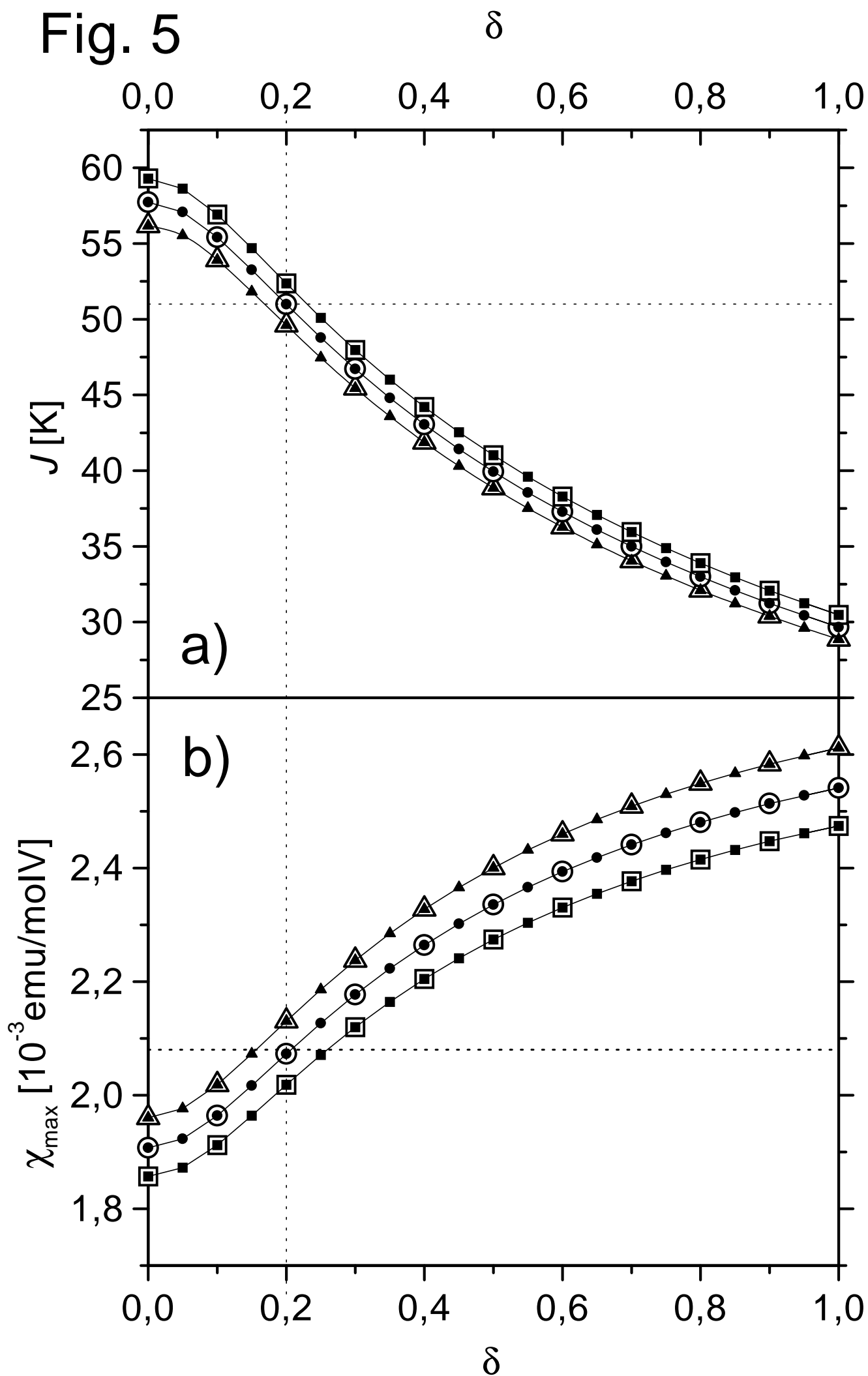


Fig. 6

